

## SSC20-III-04

## Terahertz Imaging for Space Applications

Wenschel D. Lan, Harrison K. English, Fabio D. Alves, and James H. Newman  
 Naval Postgraduate School  
 1 University Circle, Monterey, CA 93943; (831) 656 - 6275  
 wlan@nps.edu

## ABSTRACT

The Sensor Research Laboratory (SRL) at the Naval Postgraduate School (NPS) is conducting research on terahertz (THz) imaging for space applications. The approach is two-fold: a commercial-off-the-shelf long-wave infrared (LWIR) camera using uncooled microbolometer technology has been modified with THz optics; and THz-to-IR band converter focal plane arrays have been developed to work as an attachment to the IR cameras. The small form factor of these technologies has enabled the Space System Academic Group at NPS to develop a CubeSat payload based on the THz imaging camera (TIC). The objective of this technology demonstrator is to examine the potential imaging capability in the THz range in the space environment, as THz radiation can penetrate many common gases, non-polar liquids, and non-metallic solids. In preparation for an upcoming launch opportunity in 2022, confidence testing has been performed on an engineering development unit of the TIC, and a concept of operations has been developed to capture low-resolution images in both the IR and THz ranges. There is unexplored potential for THz imaging, and this mission is a first step towards enabling additional imaging capabilities for applications such as submillimeter astronomy, space situational awareness, rendezvous and proximity operations, and possibly satellite inspection.

## INTRODUCTION

Space-based imaging in the visible and infrared (IR) spectra is widely used across all mission sets, including earth-observation, weather, and space situational awareness.<sup>1</sup> IR imaging typically requires cryocooling, which is typically not accommodated on CubeSats due to size and power limitations.<sup>2</sup> Although microbolometer technology has enabled the uncooled IR imaging for terrestrial non-destructive evaluation and inspection, this is a largely unexplored space application. The advent of commercial-off-the-shelf (COTS), small form factor, long-wave infrared (LWIR) cameras based on uncooled microbolometer focal plane arrays (FPA), coupled with the terahertz-to-infrared conversion research being performed by the Naval Postgraduate School's (NPS) Sensor Research Laboratory, results in a prime candidate for developing a terahertz (THz) imaging payload by the Space System Academic Group at the NPS. An overview of terahertz imaging capabilities and the baseline spacecraft configuration will be presented, followed by a discussion of a concept of operations (CONOP) to image three potential targets for a nominal technology demonstrator mission. The results of the hardware-in-the-loop simulation of this CONOP included in this paper validate the feasibility of this mission to inform its use in future missions of interest, ranging from on-orbit inspection to submillimeter astronomy. The environmental test results verify that the COTS components are suitable for spaceflight and determine

the thermal requirements of the payload for this technology demonstration.

## Radiometry

The THz frequency band ranges from 100 GHz to 20 THz, or between approximately 1 mm and 15  $\mu\text{m}$  in wavelength. As depicted in Figure 1, the THz range is on the lower end of the IR frequency band (i.e., longer wavelength). Consequently, colder objects can be better imaged with THz sensors when compared to IR sensors. This includes LWIR, where the peak spectral irradiances occur between 193 and 362 K (-80 to 89 °C). Objects with peak spectral irradiances occurring below 150 K (-123 °C) are more likely to be detected by THz sensors. This phenomenon is shown in Figure 2 using Planck's blackbody radiation curve, where the peak frequencies are below 10 THz (marked by the green vertical line). Integration over the THz and LWIR ranges reveals that the irradiance in the THz band (0.1-20 THz) is greater than the LWIR band (20-40 THz).

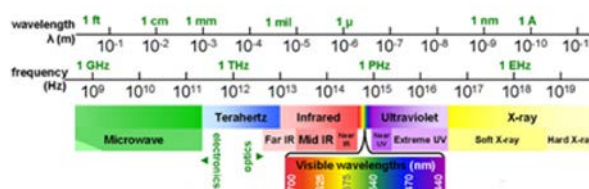
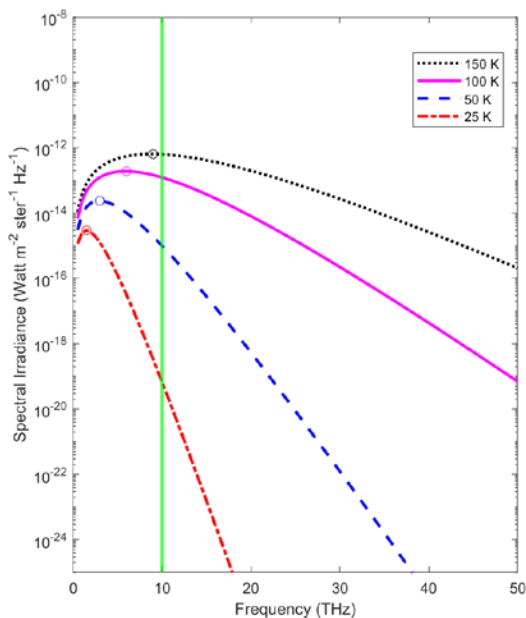


Figure 1: Electromagnetic Spectrum Depicting the THz Band<sup>3</sup>



**Figure 2: Spectral Irradiance Between 25 and 150 K (Log Scale)**

### TERAHERTZ IMAGING CAPABILITIES

THz radiation can penetrate gases, non-polar liquids, and non-metallic, solid materials such as plastics and composites. It can also be used to characterize powders and electronics. The aerospace industry has leveraged this capability most recently for non-destructive evaluation (NDE). This includes inspecting the Space Shuttle foam insulation and wind turbine blades composed of glass fiber-reinforced plastic.<sup>4, 5, 6</sup>

However, use of THz frequencies is limited terrestrially as energy within this frequency band is mostly absorbed by water vapor within Earth’s atmosphere. Due to the absence of water vapor and carbon dioxide (CO<sub>2</sub>), there is a significant potential advantage for using THz imaging in space.<sup>5</sup> For example, the interest for on-orbit servicing to extend mission lifetime<sup>7</sup> is complemented by a need for on-orbit satellite inspection. With the sun as an ideal THz source, any object illuminated by the sun can be successfully imaged, if it is within optical range. The additional imaging capability in an unexplored frequency range opens the door for rendezvous and proximity operations, as well as space situational awareness.

There are potential applications for atmospheric, weather, and astronomy observations in the THz range as well. Although submillimeter astronomy has been done from space, namely on the Submillimeter Wave Astronomy Satellite (SWAS) and the Herschel Space

Observatory, these systems are extremely complex and much larger.<sup>8</sup> The THz imaging payload developed by NPS, using microelectromechanical systems (MEMS) technology is simple, small and low cost. These properties conceivably enable novel imaging of cosmic dust and the evolution of galaxies by smaller and simpler spacecraft.

### Terahertz-to-IR Conversion

Traditional semiconductor detectors used in IR imaging require cryogenic cooling to isolate the thermal emissions of internal components on the spacecraft from the imaging target.<sup>9</sup> This results in demanding payload requirements for this capability in space—liquid nitrogen storage tanks and associated manifold or mechanical refrigerant devices become a necessity and increase the size, weight, and power (SWaP) of the spacecraft. An alternative approach is to use uncooled microbolometer IR cameras, which sense changes in temperature. While this technology is common for applications such as military night-vision systems and firefighting, the large pixel pitch restricts most commercial-off-the-shelf (COTS) arrays to 640 x 480 pixels, which limits its applications for space-based remote sensing.<sup>10</sup> However, this resolution may be acceptable for space-based imaging applications discussed thus far.

Uncooled COTS microbolometer cameras have spectral sensitivity between 8 and 14 μm, determined by the anti-reflective coating of their optics. Nevertheless, the sensing element, silicon nitride, is capable of absorbing longer wavelengths.<sup>11</sup> When the original infrared optics are replaced by lenses made of Tsurupica™, which is transparent to THz and opaque to IR<sup>12</sup>, THz energy can be detected without any conversion system.

Alves et al. demonstrated the feasibility of metamaterial-based THz-to-IR converters, fabricated with aluminum (Al) and silicon oxide (SiOx) on a silicon (Si) substrate, using standard MEMS microfabrication techniques.<sup>12</sup> These sensors were tuned to successfully absorb between 3 and 5 THz and emit wavelengths that were readable by a commercial LWIR camera. The integration of such a sensor with an IR camera to form a THz imaging camera (TIC), is conceptually shown in Figure 3. THz radiation from a hypothetical dark area of space passes through THz optics and is focused on the THz FPA. Each pixel of the array heats up proportionally to the incident THz radiation. The back side of the THz FPA is imaged by an IR camera that reveals objects that are not seen in other spectral bands.

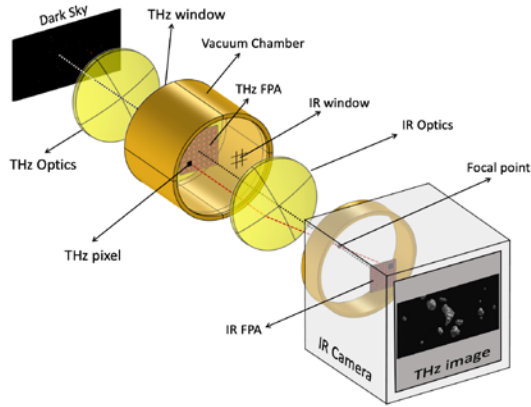


**Figure 3: Terahertz to IR Imaging System Concept**

By leveraging the small form factor, low power consumption, and high reliability<sup>13</sup> of uncooled COTS microbolometers and integrating it with state-of-the-art, THz-to-IR conversion technology, a TIC is an ideal CubeSat payload candidate for a technology demonstration mission.

**PAYLOAD DESCRIPTION**

For the first technology demonstration mission, the TIC payload will consist of two uncooled COTS microbolometer IR cameras—one that is sensitive in the THz band by way of a Tsurupica™ lens, and one that will operate in the native LWIR band camera. By flying the IR camera side-by-side with the THz camera and capturing images two seconds apart, the same scene can be recorded in both spectral bands. The IR image can be used as a reference for the THz image when analyzing the data on the ground. Many COTS uncooled microbolometer cameras are capable of detecting images in the LWIR range, but the Tamarisk 640 LWIR camera was selected due to its size; the camera base measures less than 5 cm per side. The bench setup of this nominal configuration, along with the Raspberry Pi 3A+ single-board computer (SBC) stack that will be used to control the cameras and interface with the bus, is shown in Figure 4. Two hardware-attached-on-top (HAT) daughter boards are included in the payload computer stack. The PiCapture, a COTS HAT, accommodates the use of the cameras’ analog output without the burden of in-house software requirements for data compression from the digital output. Minor modifications were made to this board to reduce the overall height of the stack and to remove non-flightworthy components. The custom RS-232 converter HAT allows for the cameras to be controlled through its RS-232 interface from the UART interface on the Raspberry Pi. Not only is this feature necessary for capturing images, but also, calibration and camera setting changes are anticipated, particularly in the event

that the sensor becomes saturated and is unable to recalibrate on its own.<sup>14</sup> This HAT also facilitates access to the 5V power rail on the Raspberry Pi, which powers both cameras. The use of the Raspberry Pi adds size and power requirements to the overall spacecraft; however, this approach was chosen to maximize launch opportunities for the TIC payload and enable early payload development efforts without identification or access to a spacecraft bus. The TIC payload has a total mass of 502 g and an average power consumption of 6.55 W when capturing an image.<sup>6</sup>

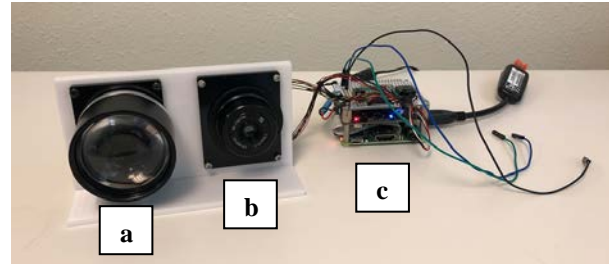


**Figure 4: TIC Payload – Nominal Bench Test Setup with a THz camera (a), the IR camera (b), and the Payload Computer Stack (c)<sup>6</sup>**

The main software for the TIC payload, or the Host Application Link (HAL), that runs on the Raspberry Pi serves two purposes—manage commands and their execution for the TIC payload and determine what spacecraft bus is being used. The latter function was developed for greater flexibility in the early payload development phase, and the former function translates the commands to communicate with the spacecraft bus. HAL constantly listens for a command, or a complete byte stream, from the UART interface. Once a complete byte stream is detected, the command is decoded using the associated JavaScript Object Notation (JSON) objects and executed. The commands developed for the TIC payload are summarized in Table 1, enabling mission and operations data to be generated, managed, and passed between the payload and the ground user.<sup>6</sup>

**Table 1: TIC Payload Commands<sup>6</sup>**

Command	Description
ping	Responds to Ping with string “Pong” and time
capture	Takes picture and automatically sends picture(s) to bus
send	Sends file specified to the bus
sendall	Sends all files in specified directory to the bus
files	Requests the filenames of the files in a directory
msg	Sends command for camera settings
linuxcmd	Sends Linux command for Raspberry Pi
delete	Delete file with specified filename
deleteall	Delete all files within a specified directory

## CONCEPT OF OPERATIONS

As the CubeSat industry continues to evolve and mature, commercial buses have become more widely available. In the spirit of “test like you fly, fly like you test”, the resulting increased reliance on commercial buses for mission success prompts the need for extensive hardware-in-the-loop, end-to-end testing on flight-like hardware and software. Astro Digital’s Corvus-6 bus was selected as the baseline bus for this mission due to its use of the Advanced Solutions, Inc. (ASI) Modular, Autonomous, eXtensible (MAX) Flight Software package. This modular flight software architecture also runs a commercial plug-in, SOLIS, in Analytical Graphics, Inc. (AGI) Systems Tool Kit (STK).<sup>15</sup> The capability to run a flight-like simulation of the entire spacecraft with incremental inclusions of payload and bus hardware and software during the development phase allowed for continued development towards a payload and mission concept of operations (CONOP).

### Baseline Spacecraft Configuration

The Corvus-6 bus is of the 6U form factor and can accommodate up to 3U of payload volume. To maximize the flight opportunity, additional payloads were included in the spacecraft configuration for this technology demonstration. One of the payloads that directly drives the requirements for the TIC payload is the X-band software-defined radio (SDR) that is being developed by NPS as an on-orbit test platform for the X-band downlink capability on the Mobile CubeSat Command and Control (MC3) network.<sup>16</sup> By considering a total 2U of volume for both payloads, this reduces the overall SWaP required, leaving 1U of volume for an additional payload that can be considered separately. The TIC payload components and the approximate volume remaining for the X-band SDR (shown in grey) are depicted in Figure 5, demonstrating the feasibility of this approach.

Combining these payloads into a single technology demonstration, with the testing strategy described above, lets the X-band SDR use the TIC payload as a data generator to test the downlink. For redundancy, the TIC payload data will nominally be sent through both the tracking, telemetry, and command (TT&C) radio on the bus as well as the X-band SDR. The data flow for the TIC payload is summarized in Figure 6, where the TIC payload is agnostic to the data downlink. A store-and-forward architecture will be employed for this mission—the TIC payload will capture and store the images locally, downloading the data to a ground station and receiving commands for clearing stored memory, resending data, or setting a new target when there is a viable pass. On average, there are between

five and ten viable passes per day across the MC3 network, currently imagined at ten ground sites during this mission. Because the ground stations are mostly located in the United States, there are ample imaging opportunities throughout the spacecraft’s orbit.

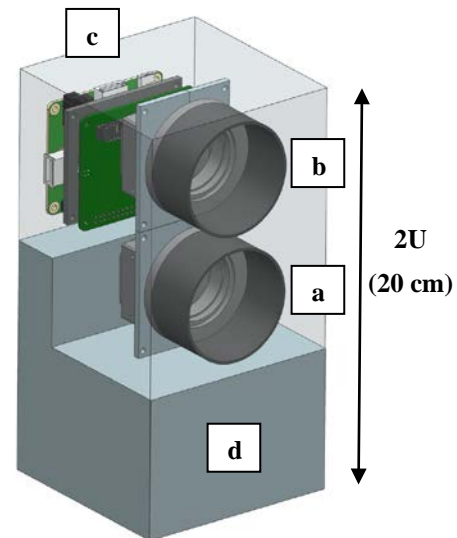


**Figure 5: TIC Payload, Consisting of THz camera (a), the IR camera (b), and the Payload Computer Stack (c), with Remaining ~1U Volume for X-Band SDR Payload (d)**

The nominal configuration of these payloads within the Corvus-6 bus, for the purposes of CONOP development, is shown in Figure 7, with the radio antennas mounted on the nadir-facing side of the spacecraft (negative Z-axis) and the TIC payload pointed out the positive x-axis. The orientation of the spacecraft with respect to the MC3 ground station at NPS is shown in Figure 7.

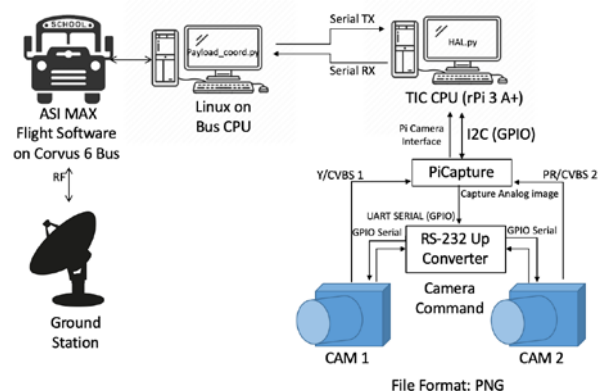


**Figure 6: TIC Payload Data Flow to Ground Station<sup>6</sup>**



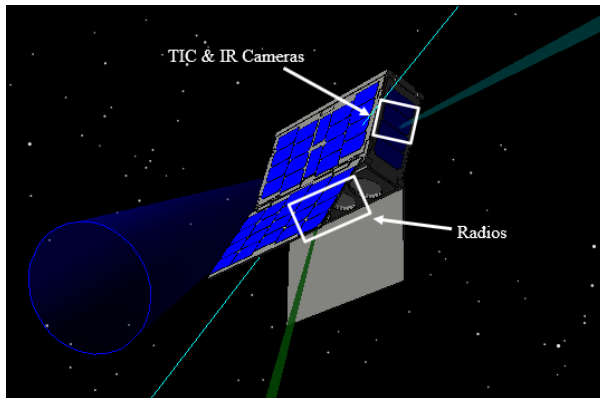


**Figure 7: Nominal Location of Payloads on Corvus-6 Bus for CONOP Development<sup>6</sup>**

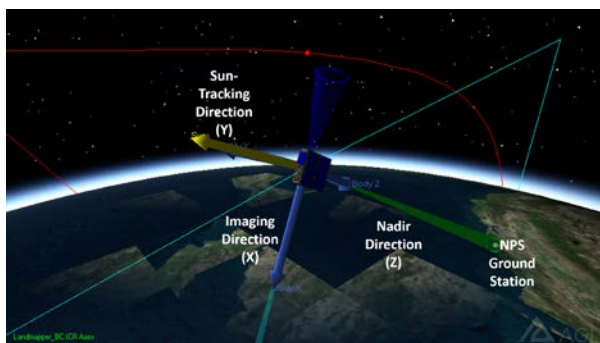


**Figure 8: Nominal Corvus-6 Bus Coordinate System, Radios Pointed at NPS MC3 Ground Station<sup>6</sup>**

### *Simulation Set Up*

The orbit parameters of this technology demonstration have not yet been determined; therefore, a sun-synchronous orbit at 500 km was used for the development of this CONOP. While the launch and initial checkout are important phases of the mission, the focus of this discussion will be on operations of the nominal TIC payload after the spacecraft has detumbled, bus health checks are complete, and initial communications have been established with the ground station. The simulation was first developed in STK without hardware in the loop; all of the system performance parameters were modeled using SOLIS. Once CONOP development was complete in STK, the C&DH EDU module with the TIC payload connected were introduced and the simulation was repeated in real-time. This setup is represented in Figure 6, where the serial transmissions are passed through the desktop computer that is running STK, and the ground station is not included in the simulation.

### *Target Sequence Description*

Three modes were considered in developing the TIC payload CONOP—ground-track, sun-track, and image targeting mode. The target sequence is time-based; however, due to the nature of the availability of imaging opportunities and ground station passes, the sun-track mode was prioritized to maintain adequate power through the mission. For the ground-track mode, the NPS MC3 ground station was chosen as the primary location and the initial target in this simulation. The spacecraft configuration will require the spacecraft to slew between each of these modes. The simulation timeline discussed here is shown in Figure 9, which illustrates the automated return to sun-track mode between image target opportunities. Four imaging targets, two in space and two on the ground, were selected for the initial set of data to be collected by the TIC payload, with the expectation that additional targets will be selected throughout the mission lifetime.

The space objects in the target sequence simulation include a co-orbiting satellite and a bright star. A spacecraft in geosynchronous orbit (GEO) was considered for this target sequence but was not included because it is unlikely that the size of the optics for this TIC payload will be able to detect the irradiance of the spacecraft from low-earth orbit (LEO). From preliminary analysis of the THz camera, it is expected that the firmament IR and THz radiation will be captured, and these space objects will appear as dots. Ground targets were also considered to better understand the payload—the reflected THz radiation on the Earth's atmosphere captured by the TIC payload is expected to provide useful data.

A co-orbiting satellite in LEO was selected to set up the target sequence, in the event that an opportunity arises to demonstrate the feasibility of any use case involving proximity and rendezvous operations. A generic satellite in the same orbit as the Corvus-6 bus, with a phase shift of 15°, was simulated for this portion of the CONOP. As this would be the closest potential target to the TIC payload, it is potentially the least taxing maneuver for the spacecraft. To deconflict this maneuver from the ground station, a 12-minute (720 seconds) separation was built into the simulation upon completion of the ground station pass.

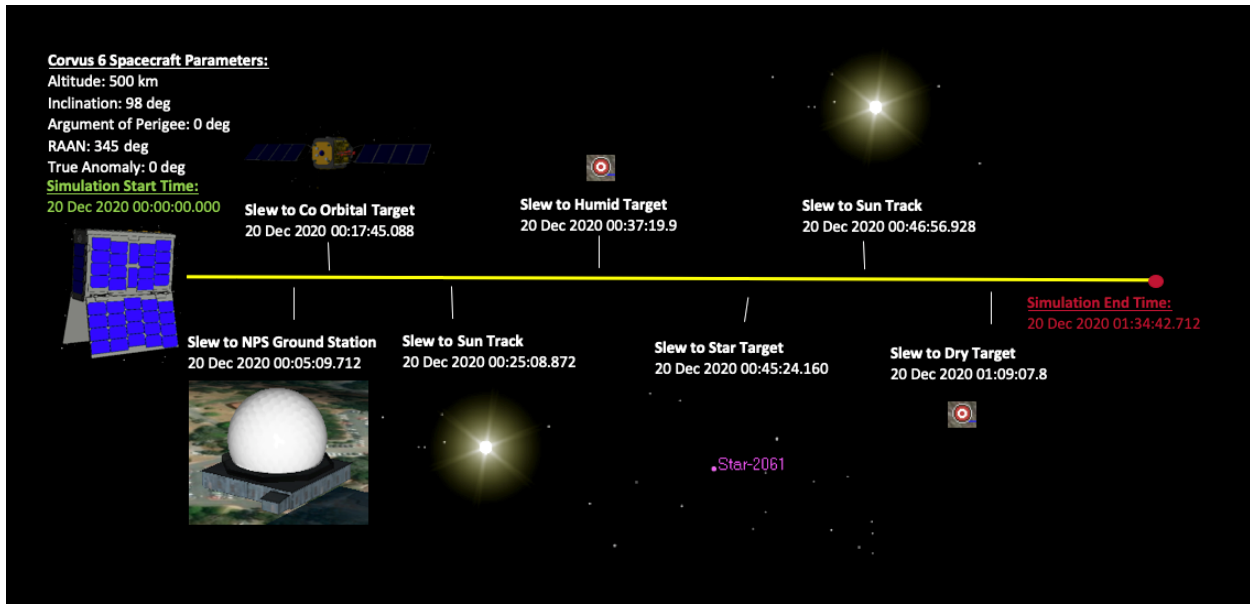


**Figure 9: Nominal Target Sequence Timeline**

Although THz energy is absorbed by water vapor and carbon dioxide, the varying levels of humidity within Earth's atmosphere may provide shades of THz energy that can be compared with weather data over the selected regions. To explore this possibility, two ground targets were selected based on their humidity and average rain fall. The first ground target selected was Rentachintala, India, with an average relative humidity of 51%, was selected as the next imaging target.

Betelgeuse, the second brightest star in the Orion constellation, was selected because of its strong spectral irradiances in the IR region.<sup>17,18</sup> Including this third target in the CONOP holds potential in submillimeter astronomy applications and facilitates the process for imaging distant objects. Betelgeuse will also be used during the initial payload checkout phase of the mission to validate that an image captured by the TIC payload is successfully received by the ground station.

To provide contrast with images of the ground target of a highly humid area, the McMurdo Dry Valleys in Antarctica were selected as the dry target for this simulation. Antarctica is one of the coldest places on Earth, and the McMurdo Dry Valleys are a 4,800 km<sup>2</sup> area that has seen no rain in millions of years.<sup>19</sup> This is the final target that was chosen for the simulation.

## TESTING

### *Functional Testing*

During the functional testing of the TIC payload, the HAL software was validated for the nominal CONOP simulated in STK SOLIS. For this testing, the set up

shown in Figure 4 connected to the TIC payload successfully captured images that were sent to the bus for storage. The images captured by the TIC payload with both the IR and THz cameras are shown in Figure 10. Due to the lack of an available THz source when the test was conducted and the presence of water vapor at ambient pressure and temperature, the image captured by the THz camera is not clear.<sup>6</sup> If a significant amount of THz energy is present, such as from a soldering iron heated to 738 K (465 °C), a clearer image of the object can be obtained. This phenomenon is depicted in Figure 11, in which an image of a hot soldering iron was captured with the THz camera at ambient temperature and pressure. It is important to highlight that the images shown in Figure 10 and Figure 11 are raw images and no processing was performed. Tremendous enhancement can be obtained with common image processing algorithms.

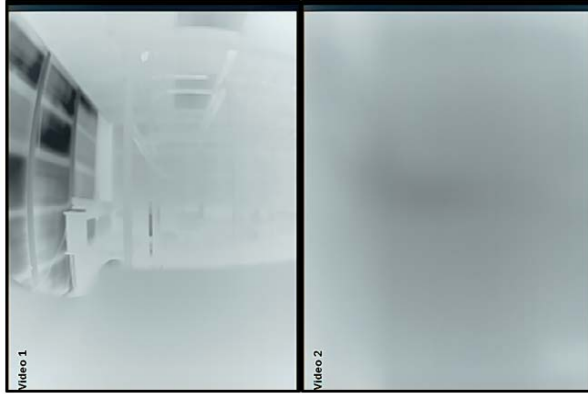


**Figure 10: Resulting Images Captured by IR Camera 1 (Left) and THz Camera 2 (Right) During Functional Test<sup>6</sup>**



**Figure 11: TIC Image of Soldering Iron at 738 K (465 °C)<sup>5</sup>**

Edge case testing was also performed, using the test setup shown in Figure 4 and the commands found in Table 1, to exercise the TIC payload software for potential failures in either one of the individual cameras or the TIC payload as a whole. Camera failure, the loss of the connection between the bus and payload, and error logging were considered. Two tests were conducted to simulate camera failures, either through a loss of connection during image capture or a camera failure prior to image capture. In both scenarios, the IR camera was disconnecting from the HAT. Two additional tests were conducted to simulate a hardware failure between the bus and the TIC payload. This was completed by disconnecting the UART cable between the payload the bus, again during a file transfer and before the command was issued. In all four tests, the software successfully entered its “debug” mode and logged an error.<sup>6</sup>

### ***Environmental Testing***

Preliminary environmental testing has been conducted on the THz camera, the Raspberry Pi 3B+, and the PiCapture to gain confidence in these COTS components for spaceflight. Vibration testing was conducted to 14.1 G<sub>RMS</sub> per the NASA General Environmental Verification Standard (GEVS), and thermal vacuum testing has been performed as well for a single cycle from -40 to 80 °C with one-hour dwells. No anomalies were encountered after vibration testing, but thermal vacuum (TVAC) testing corroborated findings that indicate the cameras will need to be recalibrated on-orbit.<sup>5, 14</sup>

### **CONCLUSION**

The potential for space-based THz imaging has yet to be realized, but the CONOP developed for the technology demonstration mission of the TIC payload highlights the possibilities. IR and THz images will be taken nearly simultaneously for comparison and data analysis that can be used for further development of this technology. Because the same software is used in both the simulation and on the command and data handling (C&DH) module of the Corvus-6 bus, NPS was able to efficiently develop the TIC payload through functional, flight-like testing in a laboratory environment. Initial testing results indicate that the focal plane array will require on-orbit calibration. Similar testing performed on THz-to-IR converter will further refine the thermal requirements for this payload.

### ***Path Forward***

Although the TIC payload is ready for flight-specific testing and integration, there are several areas of research that are required for launch readiness. End-to-end compatibility testing with the MC3 network remains, and all of the ground stations within the network need to be included in the CONOP. Additionally, the integration of a THz-to-IR converter, in addition to the use of THz optics, will be considered to improve the image quality of the THz camera. A successful mission for the first flight of the TIC payload will demonstrate whether there is potential for imaging in the THz region, unexplored by small satellites, for a wide range of missions from submillimeter astronomy to satellite inspection.

## References

1. Ball Aerospace, "Space Based Space Surveillance," Accessed May 18, 2020. [Online]. Available: [http://www.ball.com/aerospace/Aerospace/media/Aerospace/Downloads/D1910\\_\\_SBSS\\_0416.pdf](http://www.ball.com/aerospace/Aerospace/media/Aerospace/Downloads/D1910__SBSS_0416.pdf)
2. J. Olson, "CubeSat-Sized Space Microcryocooler," 33<sup>rd</sup> Annual AIAA/USU Conference on Small Satellites, Logan, UT, 2019.
3. "WSU THz-Ultrafast Photonics Website", Accessed Mar. 10, 2020. [Online]. Available: <http://www.wright.edu/~jason.deibel/intro.htm>
4. S. Kline, "Flight Qualification of a Terahertz Imaging Camera as a CubeSat Payload", M.S. thesis, Space Systems Academic Group, NPS, Monterey, CA, USA, 2018.
5. J. Kozak, "Testing, Integration, and Concept of Operations Development for a THz Imaging Camera Payload", M.S. thesis, Space Systems Academic Group, NPS, Monterey, CA, USA, 2019.
6. H. English, "Concept of Operations, Software Development, And Flight Integration Testing For A Thz Imaging Camera Payload", M.S. thesis, Space Systems Academic Group, NPS, Monterey, CA, USA, 2020.
7. "Northrop Grumman's MEV-1 servicer docks with Intelsat satellite", Accessed May 25, 2020. [Online]. Available: <https://spacenews.com/northrop-grummans-mev-1-servicer-docks-with-intelsat-satellite/>
8. G. L. Pilbratt, J. R. Riedinger, T. Passvogel, G. Crone, D. Doyle, U. Gageur, A. M. Heras, C. Jewell, L. Metcalfe, S. Ott, M. Schmidt, "Herschel Space Observatory - An ESA facility for far-infrared and submillimetre astronomy", *A&A* 518 L1 (2010), DOI: 10.1051/0004-6361/201014759.
9. J. Cha, E. Fong, "A method for estimating cryogenic cooling load in an infrared payload", *AIP Conference Proceedings* 1434, 623 (2012), DOI: 10.1063/1.4706972.
10. R. C. Olsen, *Remote Sensing from Air and Space*, Second edition. Bellingham, Washington: SPIE, 2016, p. 76.
11. S. Kurashina and N. Oda, "Bolometer Type Terahertz Wave Detector," 8,618,483, 2013.
12. F. Alves, B. Kearney, D. Grbovic and G. Karunasiri, "Narrowband terahertz emitters using metamaterial films," *Optics Express*, vol. 20, no. 19, p. 21025, 2012. Available: 10.1364/oe.20.021025.
13. M. Elbner, H. Vogt, "Reliability of microbolometer thermal imager sensors using chip-scale packaging", *Procedia Engineering* 120 (2015) 1191 – 1196.
14. M. Correa de Souza, "NPS terahertz project: IR HAB flight testing and integration," M.S. thesis, Space Systems Academic Group, NPS, Monterey, CA, USA, 2017.
15. ASI, "STK SOLIS", Accessed May 25, 2020. [Online]. Available: <http://www.go-asi.com/solutions/stk-solis/>
16. G. Minelli, et al., "The Mobile CubeSat Command and Control (MC3) Ground Station Network: An Overview and Look Ahead", 33<sup>rd</sup> Annual AIAA/USU Conference on Small Satellites, Logan, 2019.
17. EarthSky, "How far is Betelgeuse?" Accessed Apr. 14, 2020. [Online]. Available: <https://earthsky.org/astronomy-essentials/how-far-is-betelgeuse>
18. J. S. Young, J. E. Baldwin, R. C. Boysen, C. A. Haniff, P. R. Lawson, C. D. Mackay, D. Pearson, J. Rogers, D. St.-Jacques, P. J. Warner, D. M. A. Wilson, R. W. Wilson, "New views of Betelgeuse: multi-wavelength surface imaging and implications for models of hotspot generation", *Monthly Notices of the Royal Astronomical Society*, Volume 315, Issue 3, July 2000, Pages 635–645, DOI: <https://doi.org/10.1046/j.1365-8711.2000.03438.x>
19. A. Soares, "Why is Antarctica the driest place on Earth?" Accessed June 2, 2020. [Online]. Available: <https://www.experienceantarctica.com/experiences/why-is-antarctica-the-driest-place-on-earth>
20. Office of the Additional Director General of Meteorology, "Climatological Normals, 1981-2010", Accessed June 2, 2020. [Online]. Available: [http://imdpune.gov.in/library/public/1981-2010/CLIM\\_NORMALS\\_\(STATWISE\).pdf](http://imdpune.gov.in/library/public/1981-2010/CLIM_NORMALS_(STATWISE).pdf)